Project Report: Project 14

Longitudinal plane missile stabilization

Peng Mun Siew, Mengying Wang, Huaijin Yao,

Main symbols

V_{m_0} --- Missile Velocity

γ ----- Flight Path Angle

θ ------ Pitch Angle

q ------ Pitch Rate

α ------ Angle of Attack

δ ------ Elevator Deflection

m ---- Mass of missile

I_y ----- Pitch Moment of Inertia

$\bar{x}$ ------ Distance from CG to IMU Positive Forward

A_{X_0}---- Axial Acceleration Positive Forward

ρ ---- Air density

S ----- Reference Area

d ------ Reference Length

g ----- Acceleration of Gravity

Ma -- Mach Number

T -----Thrust

$C_{z\alpha_0}$ -- Pitch Force Coefficient due to Angle of Attack

$C_{z\delta p_0}$-- Pitch Force Coefficient due to Fin Deflection

$C_{m\alpha_0}$ - Pitch Moment Coefficient due to Angle of Attack

$C_{m\delta p_0}$- Pitch Moment Coefficient due to Fin Deflection

I. Introduction

A missile is a guided self-propelled projectile (guided rocket), having the capabilities to sense and correct its attitude in order to reach a predetermined target. Due to its unconstrained motion in a 3 dimensional plane, a missile have 6 degree of freedom; 3 translational motion (x, y, and z) and 3 rotational motion (roll, pitch, and yaw). Missiles are normally propelled by combusting propellants (liquid or solid) through the use of rocket engine, jet engine or other types of combustion engine, which will cause the missile to loss mass as time elapses. In this paper, the mass of the missile is assumed to remain constant and the model of the missile is linearized around its operating condition to simplify the model. In other words, the missile is modelled as a linear time invariant system. This paper focuses on designing a controller to control the lateral acceleration of the missile, when the model is subjected to time delay and zero location uncertainties.

The aim of the project is to design a missile system, which is capable of rejecting outer disturbance and reaching a predetermined lateral acceleration successfully. The response and performance of the control algorithm will be assessed using a computer simulation.

The main objective of the project is to design a control algorithm for self-stabilization and disturbance rejection for a missile system.

The equations of motion of the missile can be divided into two parts, the linear motion and rotational motion, with the specific characteristics determined by the missile aerodynamic response, propulsion, and mass properties. Simulink and Matlab coding are used to simulate the behavior of the missile under different control algorithm. The analysis of the controller performance will be divided into four parts:

- Part 1: Nominal Stability
- Part 2: Nominal Performance
- Part 3: Robust Stability
- Part 4: Robust Performance

During the nominal stability analysis, the stability of the nominal plant using the designed controller is analyzed. After ensuring that the system is nominally stable, the performance of the closed loop system is analyzed to ensure that it is able to satisfy our design requirements. After satisfying both the nominal stability and nominal performance, the stability of the system when subjected to model uncertainty is analyzed, before analyzing its performance under the effect of

model uncertainties. The controller is tweaked and redesigned if any of the requirements are not met.

II. Mathematical Model

Three different coordinate frames are used in the modelling of the missile. The first coordinate frame is an inertial or ground fixed coordinate frame. The second frame is the velocity coordinate frame, where the velocity acts along the positive x' direction. The flight path angle γ is defined under these two coordinates, as shown in figure 1. The other frame is the body fixed coordinate frame, which is used to determine the angle of attack α and the pitch angle θ. The difference between the two angles above is the angle of attack with a symbol of α**.** We use q to represent the time derivative of pitch angle, θ, i.e., the pitch rate.

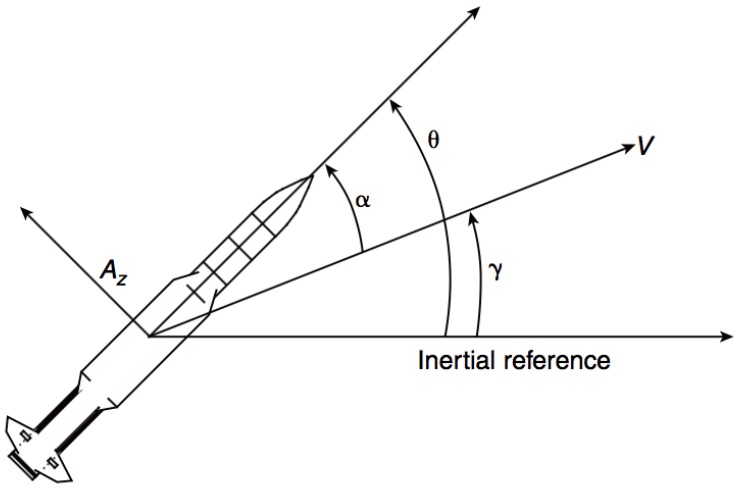

Figure 1. Angle of Attack and Pitch Angle [1]

The short period approximation of the longitudinal equations of motion of the missile [2] is used, with the states being the angle of attack, α and the pitch rate, q. The equation of motion of the system are as shown below.

$$\dot{\alpha} = f_1 = \frac{cos\alpha}{mV} F_z + q \quad (1)$$

$$f_1 = \frac{cos\alpha}{mV}\left[sgn(\alpha)\left(n_3|\alpha|^3 + n_2\alpha^2 + \left(n_{1,a} + n_{1,b}Ma\right)|\alpha|\right) + n_0\delta\right]QS + q \quad (2)$$

$$\dot{q} = f_2 = \frac{M_y}{I_y} \quad (3)$$

$$f_2 = \frac{1}{I_y}\left[sgn(\alpha)\left(m_3|\alpha|^3 + m_2\alpha^2 + \left(m_{1,a} + m_{1,b}Ma\right)|\alpha|\right) + m_0\delta\right]QSd \quad (4)$$

Using the state space notation, the basic missile longitudinal plant can be represented as followed,

$$\begin{aligned} \dot{\delta_x} &= A\delta_x + B\delta_u \\ y &= C\delta_x + D\delta_u \end{aligned} \quad (5)$$

Where,

$$\delta_x := \begin{bmatrix} \alpha - \alpha_{trim} \\ q - q_{trim} \end{bmatrix} \qquad \delta_u := [\delta - \delta_{trim}] \qquad y := [a_z - a_{ztrim}]$$

The A, B, C, D matrices can be obtained by using equation 1 to 4 above.

$$A = \begin{bmatrix} -\frac{sin\bar{\alpha}}{m\cdot a\cdot\overline{Ma}}\left[n_3|\bar{\alpha}|^3 + n_2\bar{\alpha}^2 + \left(n_{1,a} + n_{1,b}\overline{Ma}\right)|\bar{\alpha}| + n_0\bar{\delta}\right]\cdot 0.7\rho(\overline{Ma})^2S + \frac{cos\bar{\alpha}}{m\cdot a\cdot\overline{Ma}}\left[3n_3|\bar{\alpha}|^2 + 2n_2\bar{\alpha} + \left(n_{1,a} + n_{1,b}\overline{Ma}\right)\right]\cdot 0.7\rho(\overline{Ma})^2S & 1 \\ \frac{1}{I_y}0.7\rho(\overline{Ma})^2Sd\left[\left(3m_3|\bar{\alpha}|^2 + 2m_2\bar{\alpha} + \left(m_{1,a} + m_{1,b}\overline{Ma}\right)\right)\right] & 0 \end{bmatrix}$$

$$B = \begin{bmatrix} \frac{cos\bar{\alpha}}{m\cdot a\cdot\overline{Ma}}0.7\rho(\overline{Ma})^2Sn_0 \\ \frac{1}{I_y}0.7\rho(\overline{Ma})^2Sdm_0 \end{bmatrix}$$

$$C = \left[\frac{\pi}{180mg}0.7\rho(\overline{Ma})^2S\left[3n_3|\bar{\alpha}|^2 + 2n_2\bar{\alpha} + \left(n_{1,a} + n_{1,b}\overline{Ma}\right)\right] \quad 0\right]$$

$$D = \frac{\pi}{180mg}0.7\rho(\overline{Ma})^2Sn_0$$

The numerical data is attached in Appendix A, the calculated values of the matrices are as shown:

$$A = \begin{bmatrix} -0.9531 & 1 \\ -101.8547 & 0 \end{bmatrix} \qquad B = \begin{bmatrix} -0.1203 \\ -130.8664 \end{bmatrix}$$

$$C = [-1.6292 \quad 0] \qquad D = -0.2038$$

With the equilibrium point as listed in the table 1[3] below:

Name	Symbol	Value	Unit
Mach	$\overline{Ma}$	3	---
Angle of Attack	$\bar{\alpha}$	0.10472	rad
Pitch Rate	$\bar{q}$	0.0232	rad/sec
Deflection	$\bar{\delta}$	0.02976	rad

Table 1: Equilibrium Points

The open loop transfer function is given by equation

$$G(s) = \frac{-0.2038s^2 + 0{,}001751s + 192.4}{s^2 + 0.9531s + 101.9} \quad (6)$$

III. Nominal Plant

Based on the dynamic model obtained from previous section, the time delay due to the actuator dynamics was neglected in the development of the plant transfer function. The time delay of the actuator dynamics can be modelled to be within the range of $\tau \in [0\ ,0.003]$. Hence, a nominal transfer function is taken by taking the average of the time constant for the time delay and using a first order Pade approximation. The nominal plant with Pade approximation is as shown in equation 7 below.

$$G_0(s) = G(s) * \frac{-\tau s + 2}{\tau s + 2} = \frac{0.0003057s^3 - 0.4076s^2 - 0.2852s + 384.9}{0.0015s^3 + 2.001s^2 + 2.059s + 203.7} \quad (7)$$

The poles of the nominal plants are listed table 2 below.

Pole location
-1333.0
-0.5+10.1i
-0.5+10.1i

Table 2: Nominal plant open loop poles

All the poles of the nominal plant are located in the left hand plane. Thus, the nominal plant is stable. The step response of the nominal plant is shown in figure 2 and its bode plot is shown in figure 3.

Although the nominal plant is stable, the performance (transient response) are not satisfactory. From the step response, it is observed that the small damping ratio of the nominal plant causes oscillations in the response with a large settling time, which is not acceptable. From the bode plot, the gain margin and phase margin of the nominal system are relatively small, thus it does not have good robustness. Furthermore, the peak around 10 rad is not desired, for good performance, the peak need to be damped. Hence, a suitable controller need to be designed to compensate for the lack of robustness and poor performance.

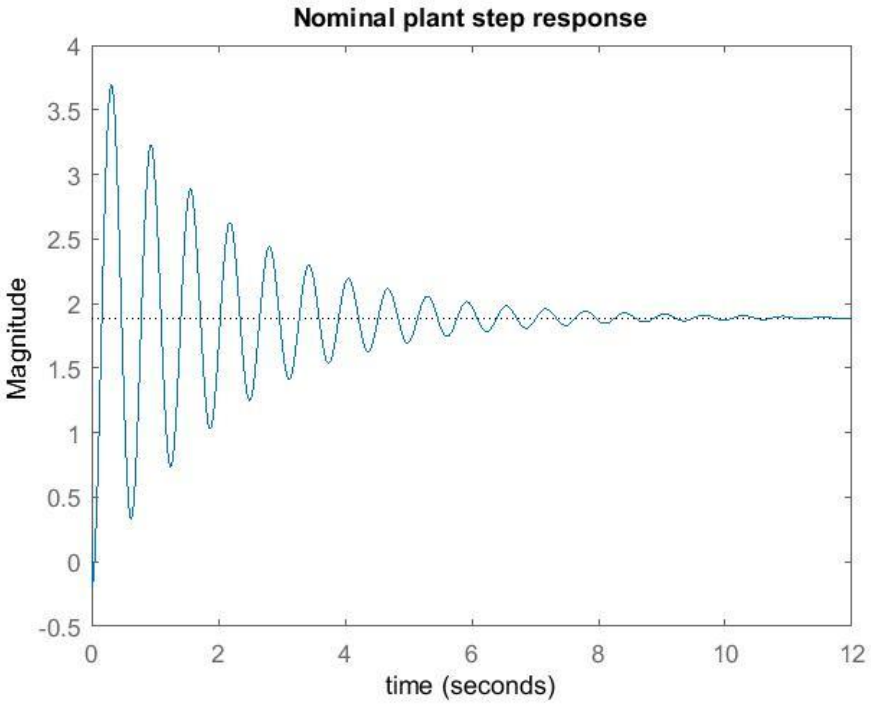

Figure 2: Nominal plant step response

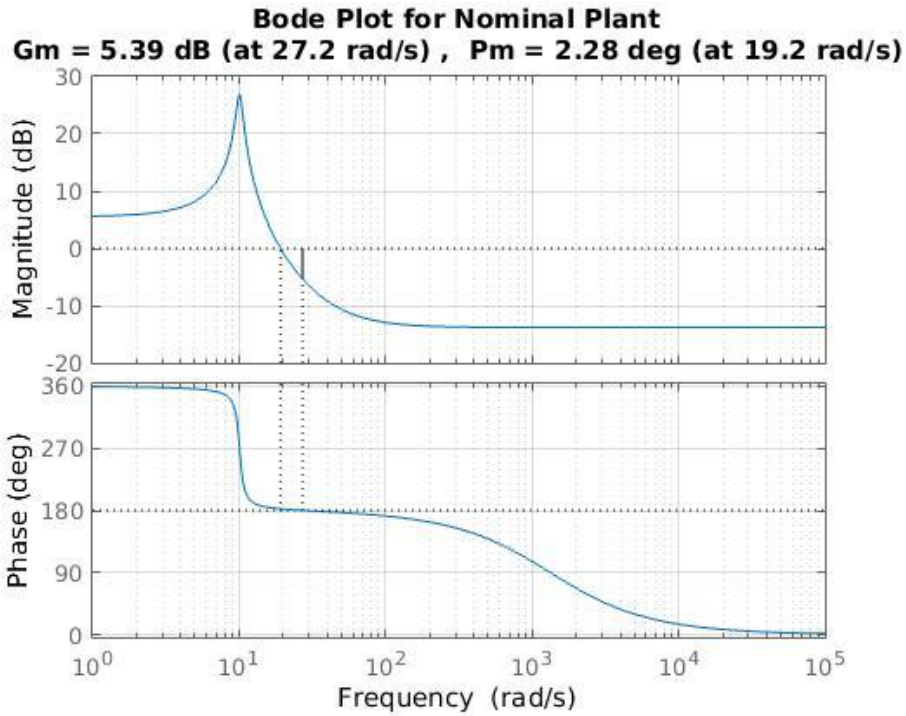

Figure 3: Nominal plant bode plot

For controller design, the mixed sensitivity controller design method is used to shape the sensitivity function as well as the complementary sensitivity function of the closed-loop system, such that it achieves the design targets of good performance and robustness. This approach is shown in details in the next part.

IV. Implementation-Mixed Sensitivity Controller Design

For a standard feedback loop, where G represents the plant and K represents the controller. The system is also subjected to an input disturbance, d_I and an output disturbance, d_o, as shown in figure 4 below.

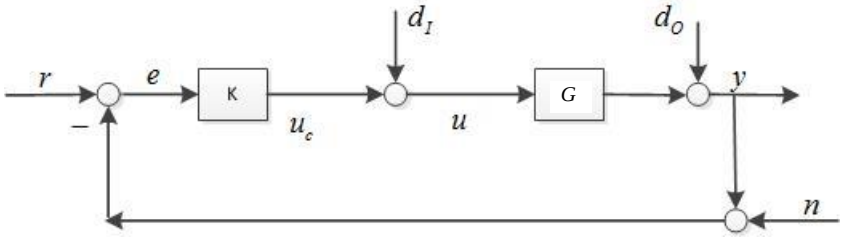

Figure 4: Standard feedback loop

The transfer function from d_o to y are as shown in equation 8 and 9 below, where $S_0 = [I + G(s)K(s)]^{-1}$ is called the output sensitivity function.

$$Y(s) = D_0(s) - G(s)K(s)Y(s) \quad (8)$$

$$Y(s) = [I + G(s)K(s)]^{-1}D_0(s) \quad (9)$$

While the transfer function from d_I to u are as shown in equation 10 and 11 below, where $S_I = [I + K(s)G(s)]^{-1}$ is called the input sensitivity function.

$$U(s) = D_I(s) - K(s)D(s)U(s) \quad (10)$$

$$U(s) = [I + K(s)G(s)]^{-1}D_I(s) \quad (11)$$

Similarly, we can then write out the input and output complementary sensitivity and loop transfer functions:

$$T_I(s) = K(s)G(s)[I + K(s)G(s)]^{-1} \quad (12)$$

$$T_O(s) = G(s)K(s)[I + G(s)K(s)]^{-1} \quad (13)$$

$$L_I(s) = K(s)G(s) \quad (14)$$

$$L_o(s) = G(s)K(s) \quad (15)$$

In a SISO case, the input and output sensitivity and their corresponding complementary sensitivity are the same, whereas for a MIMO system, they are usually different.

Assuming that the nominal plant is G and the uncertain plant is G_p, the multiplicative output uncertainty can then be defined as

$$G_P = G(I + W_O\Delta_O);\ \|\Delta_O\|_\infty < 1 \quad (16)$$

In a standard unity feedback loop shown in figure 5, the sensitivity function, complementary sensitivity and transfer function from input to actuation signal are as followed

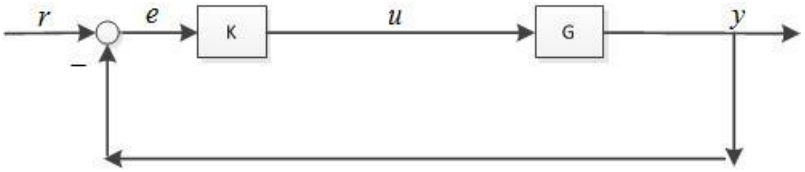

Figure 5: Standard unity feedback loop diagram

$$S_O = transfer\ function\ from\ r \to e$$

$$T_O = transfer\ function\ from\ r \to y$$

$$KS_O = transfer\ function\ from\ r \to u$$

For the system to have robust stability, our goal is to design a controller K that not only stabilizes the nominal plant G, but also stabilizes all the uncertain plant G_p. To achieve this goal, the mixed sensitivity controller design method was used.

Under the mixed sensitivity controller design method, two weights are introduced to describe the performance objectives, w_{perf}, the uncertainty weightage, w_I, and the actuator weightage, w_U. These weights serve to penalize the controller such that the response (performance, stability and actuator effort) would always lie bounded within the three weights.

w_{perf}: Good performance $\Longrightarrow |S_O| < 1/|w_p|$

w_T: Robust stability $\Longrightarrow |T_O| < 1/|w_T|$

w_U: Acceptable actuator effort $\Longrightarrow |KS_O| < 1/|w_U|$

After the addition of the weights, the system will have a form as shown in figure 6 below, where,

$$w_{Perf}S_O = transfer\ function\ from\ r \to \tilde{e}$$

$$w_T T_O = transfer\ function\ from\ r \to \tilde{y}$$

$$w_U KS_O = transfer\ function\ from\ r \to \tilde{u}$$

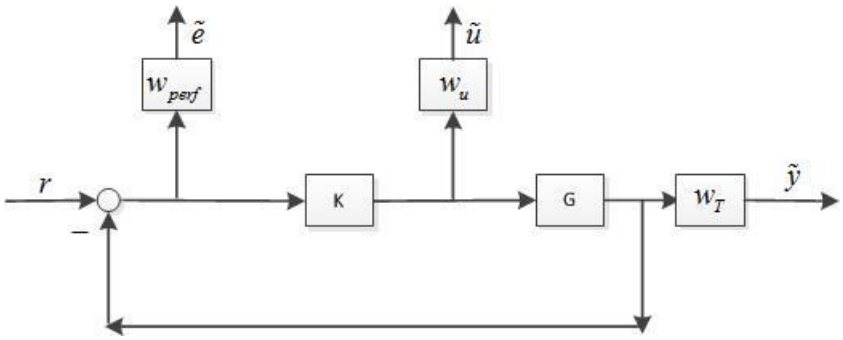

Figure 6: Loop diagram with weightage

Following the above description, the mix sensitivity design can be interpreted as minimizing the gain from reference, r to the error, controller effort and the output.

$$r \rightarrow \begin{bmatrix} \tilde{e} \\ \tilde{y} \\ \tilde{u} \end{bmatrix} \tag{17}$$

For the mixed sensitivity design, these requirements are combined into a H_∞ constraint and the controller K is designed such that it minimizes the H_∞ norm:

$$H_\infty = \left\| \begin{matrix} w_s S_O \\ w_T T_O \\ w_U K S_O \end{matrix} \right\|_\infty \tag{18}$$

$$\min_{K \in S} \gamma$$

$$\text{Subjected to } \|H_\infty\| < \gamma$$

If $\gamma^* \leq 1$, then the design requirements are met. In our design, the control effort weightage was not used as the top priority is to satisfy the performance and stability requirements.

In general interception [5], the time constant should be less than 0.7s.

For the system to be stable when subjected to model uncertainties, a gain margin and phase margin [6] of no less than 6dB and 30° is desired.

For performance index, choose both indexes in time domain and frequency domain, the chosen performance index is listed in table 3.

Name	Symbol	Value
Time constant	τ	< 0.7 s
Damping ratio	ξ	1
Crossover frequency	ω_c	5 rad/s
Steady state error	--	<1%

Table 3: Performance Index

Design of w_{perf}:

For our case, the performance weighting function, w_{perf} is proposed with the following expression. The sensitivity transfer function will be bounded by the inverse of the performance weighting function.

$$w_{perf} = \frac{\alpha s + \omega}{s + \beta\omega} \quad (19)$$

The variable α is the high frequency gain of the weight function. Typically, the maximum peak of the magnitude of S_o is about 2 for acceptable system response, therefore an upper bound is imposed on S_o using the high frequency gain of the performance weighting function, α. Consequently, an appropriate value for α should be approximately 0.5. In our design case, an α of 0.5 is chosen.

The variable β is the weighing function gain at low frequency. This value is related to the upper bound on the allowable steady state error. For ideal cases, null steady state error are desired, which corresponds to the value of β being zero. However, when solving the problem numerically, we cannot select β as zero, so an appropriate small value of β is used based on the design requirement.

From performance index, the steady state error should be less than 1%, therefore a value of 0.01 is chosen.

The ω is the crossover frequency of the function. This value indicates the minimum bandwidth of the transfer function which are weighted. Based on the performance index listed in table 3, we choose our bandwidth to be at 5 rad/s.

Summarizing the weighting function parameters in table 4:

Variable	Value
α	0.5
β	0.01
ω	5

Table 4: Weighting function parameters

The Matlab function 'makeweight' is used to construct the performance weight transfer functions. The transfer function for the performance weight is as shown in equation 20.

$$w_{perf} = \frac{0.5s + 12.99}{s + 0.1299} \quad (20)$$

The magnitude bode plot of w_{Perf} is as shown in figure 7.

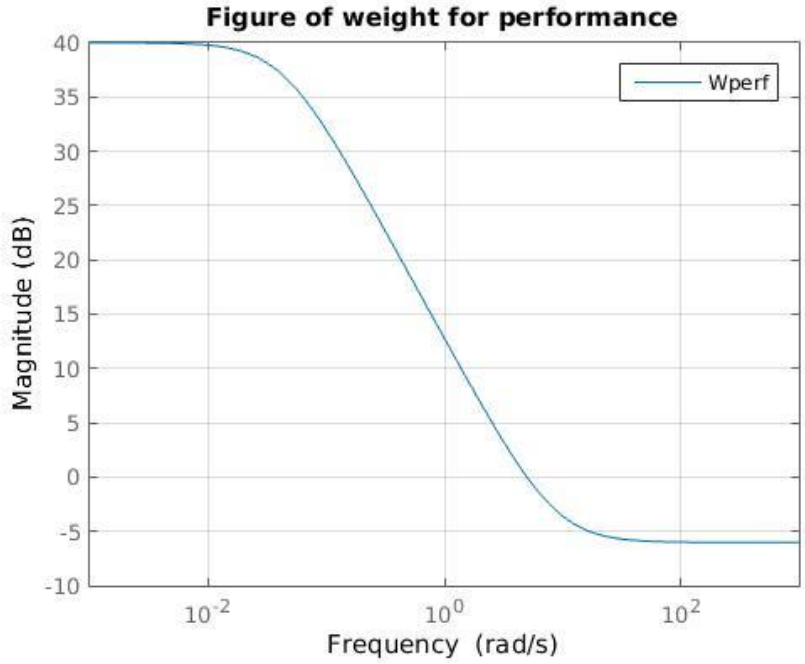

Figure 7: Bode Plot for performance penalty and control penalty weights

After determining all the weight functions, we use the H_∞ mixed sensitivity (mixsyn) design method to achieve the bounding requirements. Then the transfer function of the controller we get due to the mixsyn design is:

$$\mathrm{Kms(s)} = \frac{0.27816(s+1319)(s+787.5)(s^2+0.9531s+101.9)(s^2+2229s+2.534*10^6)}{(s+30.73)(s+0.0433)(s^2+931.6s+3.244*10^5)(s^2+2388s+2.494*10^6)} \quad (21)$$

V. Nominal Stability

For nominal stability, the closed loop poles of the system need to be located in the left half plane. The closed loop poles are as shown in table 5.

Complex conjugates poles		Real poles
positive imaginary	negative imaginary	-0.043303
-0.47655+10.081i	-0.47655-10.081i	-10.116
-435.16+98.912i	-435.16-98.912i	-30.725
-1154+1025.8i	-1154-1025.8i	-787.5
-1114+1136.9i	-1114+1136.9i	-1747.1

Table 5: Closed loop poles

As all the closed loop poles are located in the left half plane, the nominal plant is stable.

From figure 8, the step input time response of output acceleration a_z converges to a steady state value as time increases, which also verifies the stability of the closed loop system.

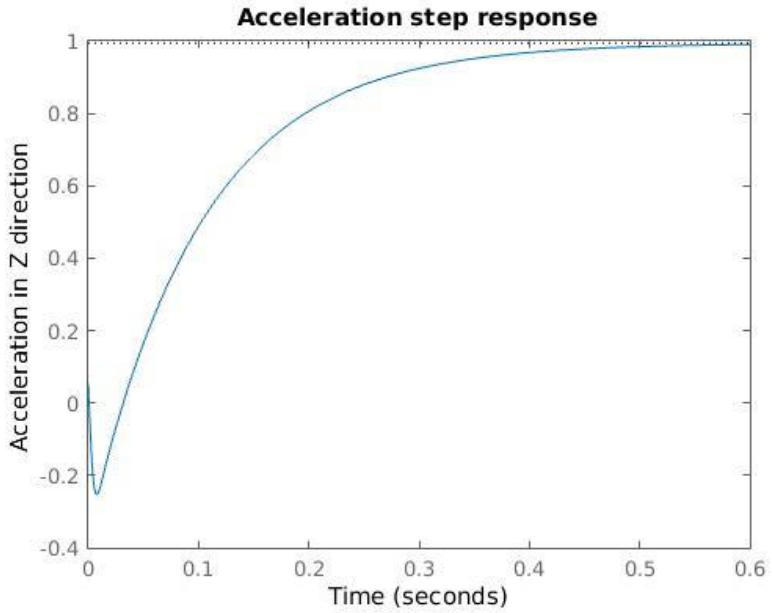

Figure 8: Step input response for Lateral Acceleration

Note that in the step input response, we have an undershoot in this plot. The reason why this undershoot shows up is that recall in equation 21, we have a non-minimum phase (NMP) zero in our controller. But as we check all the closed loop poles are all in right half plane, and in our controller design, we don't make any right half plane zero-pole cancellation, so this NMP zero will not make an influence in our nominal stability.

Another method to analyze nominal stability is by plotting the Nyquist plot of the open loop transfer function, which is shown in figure 9. The Nyquist contour plot never encircles the critical point (-1,0). From part II, the nominal plant has 0 poles in right half plant, therefore according to the Nyquist stability criteria, the feedback system is stable.

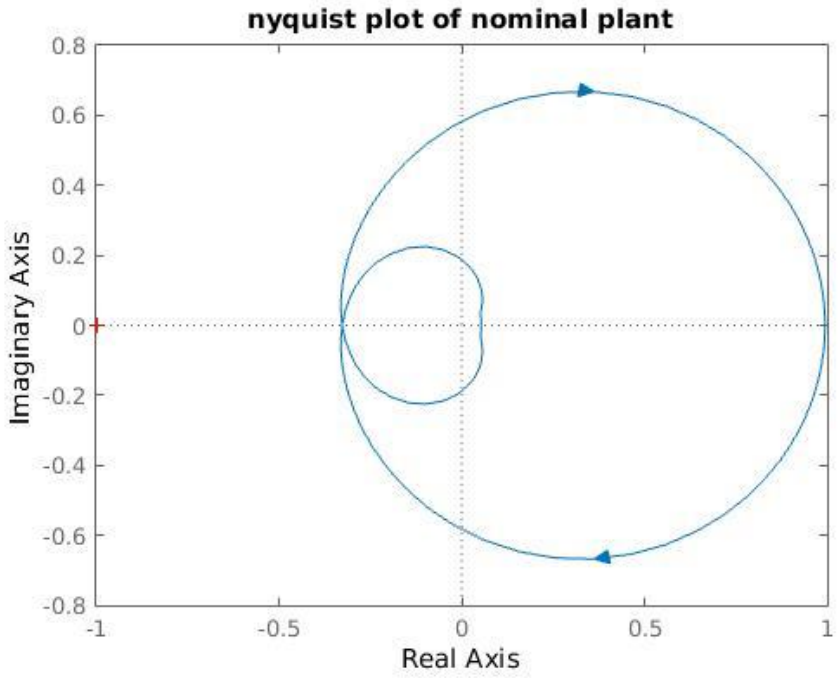

Figure 9: Nyquist plot of open-loop transfer function

VI. Nominal Performance

The nominal performance of the system is first analyzed in the time domain. From the time response plot in figure 8 in section V, the performance of the system is shown as follow:

Rise time, $t_r = \ 0.2172s$

Settling time, $t_s = 0.3983$s

The plot indicates that the performance in time domain satisfy our requirement.

The nominal performance is then analyzed in the frequency domain. The performance of the closed loop system are characterized by the specifications imposed on the frequency domain magnitude of the sensitivity function [7], that is, on $|S(j\omega)| = |1 + L(j\omega)|$. Thus, the nominal performance (NP) is defined by

$$\text{NP: } |S(j\omega)| < \frac{1}{|\omega_P(j\omega)|}, \forall\omega, \quad \Rightarrow \quad |\omega_P(j\omega)S(j\omega)| < 1, \forall\omega \qquad (22)$$

where $\omega_P(s)$ is a specified weighting function. The assumption here is that the time domain specifications, such as overshoot and settling time, or frequency domain specifications, such as phase margin and bandwidth, can be achieved by a proper choice of $\omega_P(s)$. The peak magnitude of $|S(j\omega)|$, the closed-loop bandwidth defined in terms of $|S(j\omega)|$and the low-frequency slope of $|S(j\omega)|$ is then chosen through $\omega_P(s)$.

Using w_{perf} derived from the previous section as $\omega_P(s)$.

$$\omega_P(s) = w_{perf} = \frac{\alpha s + \omega}{s + \beta\omega} \quad (23)$$

The values for M and A are α= 0.5 & β = 0.01.

For nominal performance, we should achieve $|S| < |1/W_p|$or all frequencies. $|1/W_p|$ and $|S|$ are then plotted in the same bode plot to check for nominal performance. From the bode plot in figure 10 below, we can see that the magnitude plot for the inverse of the performance weightage always encompasses the sensitivity function, which indicates nominal performance.

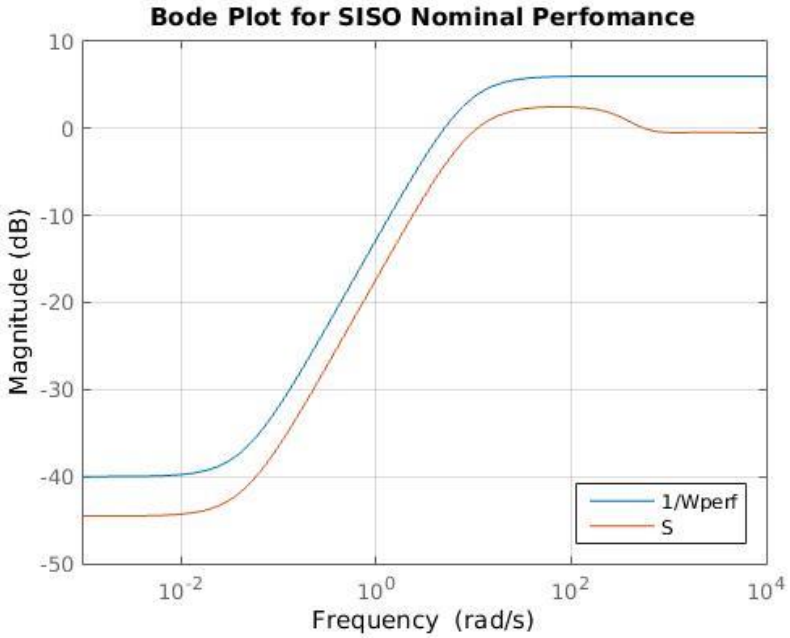

Figure 10: Magnitude bode plot of $1/W_{perf}$ and S

The magnitude bode plot of complementary sensitivity T and sensitivity S are shown in figure 11. The complementary sensitivity function rolls off at high frequency, which satisfy our requirements for high frequency noise rejection.

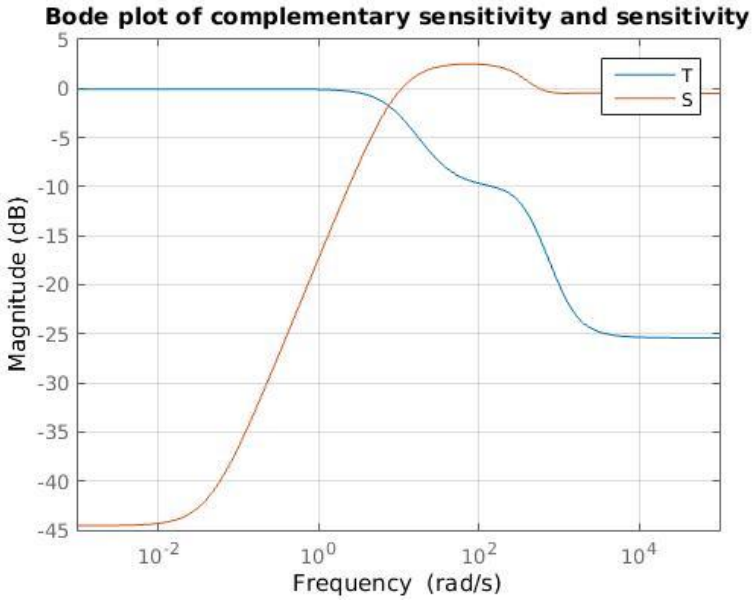

Figure 11: Sensitivity and complementary sensitivity magnitude plot

VII. Modelling of Plant Uncertainties

Time delay uncertainty: The nominal plant with Pade approximation is as shown in equation 24, where the Pade approximation was derived from a time delay of the actuator dynamics within the range of $\tau \in [0\ ,0.003]$.

$$G_0(s) = G(s) * \frac{-\tau s + 2}{\tau s + 2} = \frac{0.0003057s^3 - 0.4076s^2 - 0.2852s + 384.9}{0.0015s^3 + 2.001s^2 + 2.059s + 203.7} \quad (24)$$

Parametric Zero Uncertainty: A zero uncertainty is also added to the system with an uncertainty range of $k \in [-10,10]$ to compensate for any modelling errors. The plant with all the disturbance will be discussed in the following section.

Multiplicative uncertainty is used to analyze and represent these uncertainties. The range of all possible G_Δ is first identified using equation 25.

$$G_\Delta(\omega) = \max_{G_p \in \Pi} \left| \frac{G_p(j\omega) - G(j\omega)}{G(j\omega)} \right| \quad (25)$$

A rational weight is then used to represent G_Δ, the magnitude of the rational weight need to be greater than G_Δ at all frequencies.

$$|W_I(j\omega)| \geq G_\Delta(\omega), \forall \omega \quad (26)$$

A first order weight, W_I is first constructed using the weight function equation with n=1 (equation 27).

$$W_I(s) = \frac{(\tau * s + r_0)^n}{\left(\frac{\tau}{r_\infty} * s + 1\right)^n} \quad (27)$$

A weighting function with $r_\infty = 2.1$, $r_0 = 0.35$, and the frequency where the relative uncertainty reaches 100% approximately at $1/\tau = 375 rad/s$ was used in our first design, however this does not fully encompasses the whole uncertainty region especially near the crossover frequency. Figure 12 shows the first design W_I and the nominal plant.

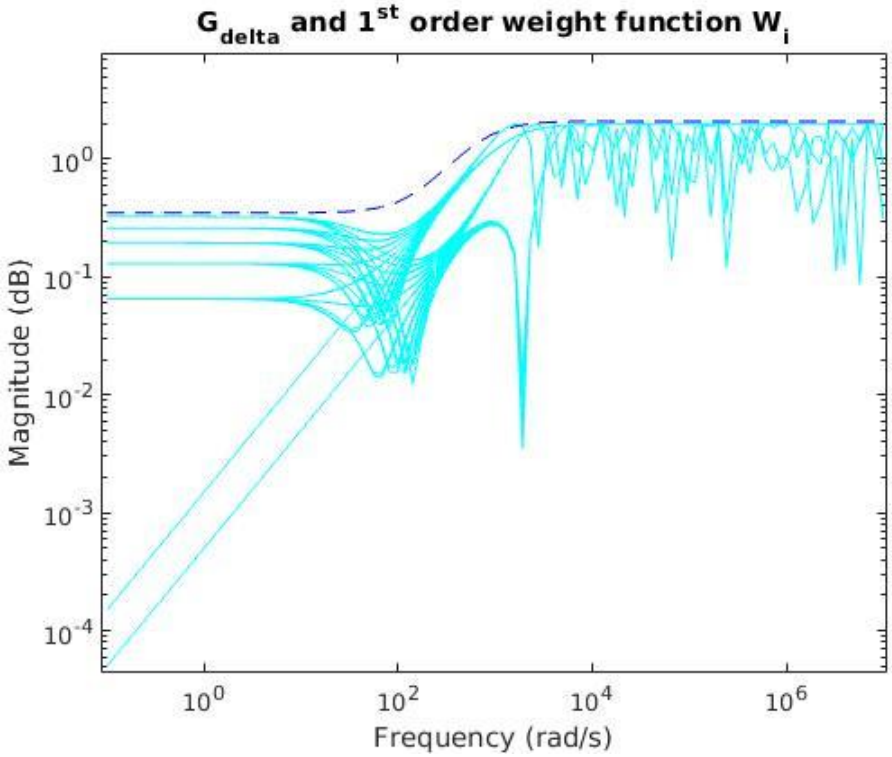

Figure 12: All possible sets of G_{delta} with the uncertainty and the 1st order weight function

Hence, a second order correcting factor is used to lift the gain slightly at the crossover frequency. The following equation works well:

$$W_I(s) = W_{1I}(s)\frac{(s^2 + 1.6 * s * \omega + \omega^2)}{(s^2 + 1.6 * s * \omega + \omega^2)}$$

Thus the final function of W_I is shown in equation 27 below, with a selected frequency$\omega = 1592 rad/s$.

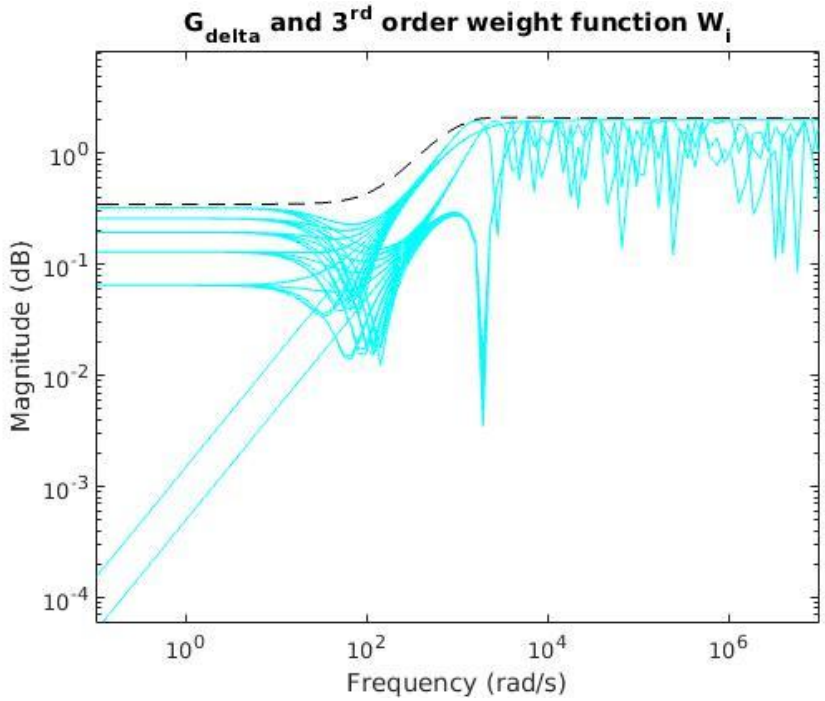

Figure 13: All possible sets of G_{delta} with the uncertainty weightage bound

$$W_I(s) = \frac{(s + 375 * 0.35) * (s^2 + 1.6 * s * \omega + \omega^2)}{\left(\frac{s}{2.1} + 0375\right)(s^2 + 1.6 * s * \omega + \omega^2)} = \frac{2.1(s + 131.2)(s^2 + 2388s + 2.534 * 10^6)}{(s + 787.5)(s^2 + 2229s + 2.534 * 10^6)} \quad (28)$$

The magnitude bode plot of G_Δ with all the possible time delay and zero uncertainty is shown in figure 13. The dash line represents the third-order weight W_I, which is used to bound all the possible G_Δ.

VIII. Robust Stability

As discussed in the earlier chapter, a nominal plant was used in our controller design, however the nominal plant might not be the exact model for our system, hence a weighting for complex uncertainty is used to represent all the possible set of plant with the parametric uncertainties covered in chapter VII.

First, the gain margin and phase margin of the loop transfer function from the elevator deflection to change in lateral acceleration is checked using Matlab and the bode plot and margin plots of the

system are as shown below. The gain margin is more than 6dB and phase margin over 45 degrees, which satisfy our desired value.

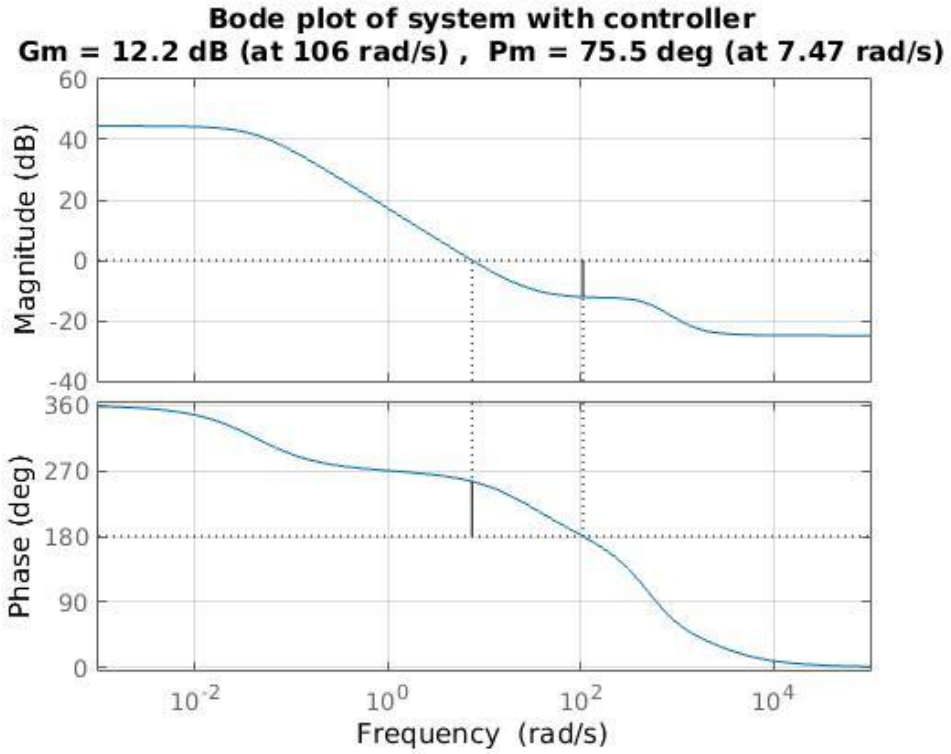

Figure 14: Bode plot of system with controller (loop transfer function)

The bode plot of the open loop system $L(s) = G(S) * k(S)$ is show in figure 14. The transfer function of L(s) is

$$L(s) = \frac{0.05669s^6 + 168.4s^5 + 1.358 * 10^5 s^4 - 1.954 * 10^8 s^3 - 4.23 * 10^{11} s^2 - 1.858 * 10^{14} s + 6.114 * 10^{15}}{s^6 + 4505s^5 + 8.854 * 10^6 s^4 + 8.727 * 10^9 s^3 + 4.042 * 10^{12} s^2 + 8.421 * 10^{14} s + 3.646 * 10^{13}} \quad (29)$$

For the system to be robustly stable, the complementary sensitivity function of the plant need to be bounded by the inverse of the uncertainty weighting at all frequency.

$$|T(s)| = \frac{1}{|W_i(s)|} \quad (30)$$

The designed controller was able to fulfill this requirement as shown in figure 16 below. This shows the ability of the controlled system to be robustly stable even when subjected to perturbations from the nominal plant.

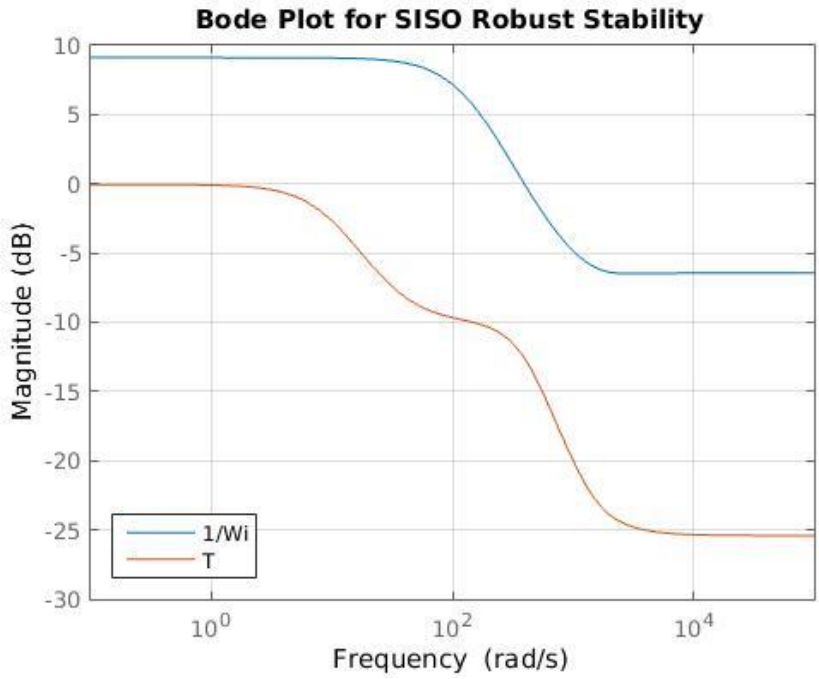

Figure 15: Bode Plot for T and 1/Wi

IX. Robust Performance

After ensuring that our designed system is able to achieve nominal stability, nominal performance and robust stability, the next analysis would be to determine whether our designed controller is still able to achieve our desired performance even when the system is subjected to uncertainties. This analysis will be conducted using two different methods:

- Method 1: Analysis from a Single Input Single Output (SISO) case perspective
- Method 2: Analysis using structured singular value (μ)

Method 1: SISO case perspective

Using a SISO case perspective, the uncertainty weightage and performance weightage can be visualized to be a disc of radius $|W_i L(j\omega)|$ and $|W_p(j\omega)|$ respectively. For a system to have robust performance, it is necessary that all possible loop transfer function, $L_p(j\omega)$, stay outside a disc of radius $|W_p(j\omega)|$ centered on -1. As the possible loop transfer function at each frequency stays within a disc of radius $|W_i L(j\omega)|$ centered on $L(j\omega)$, therefore it is necessary that the two discs

do not overlap for the system to satisfy the robust performance requirement. As their centers are located $|1 + L(j\omega)|$ apart, the RP condition becomes:

$$RP \Leftrightarrow |W_i L(j\omega)| + |W_p(j\omega)| < |1 + L(j\omega)|, \quad \forall\omega \tag{31}$$

$$\Leftrightarrow |W_i L(1+L)^{-1}| + |W_p(1+L)^{-1}| < 1, \quad \forall\omega$$

$$RP \Leftrightarrow max_\omega\left(|W_i T| + |W_p S|\right) < 1 \tag{32}$$

The magnitude plot of $|W_i T| + |W_p S|$ is then constructed for all frequency as shown in figure 16 below. This magnitude need to be below 1 for all frequency for the system to achieve robust performance. For our system, the highest magnitude is at frequency lower than 1 rad/s with a magnitude of 0.938, hence our designed controller is able to achieve robust performance.

For our system,

$$max_\omega\left(|W_i T| + |W_p S|\right) = 0.94 < 1$$

Hence, the robust performance criteria is satisfied.

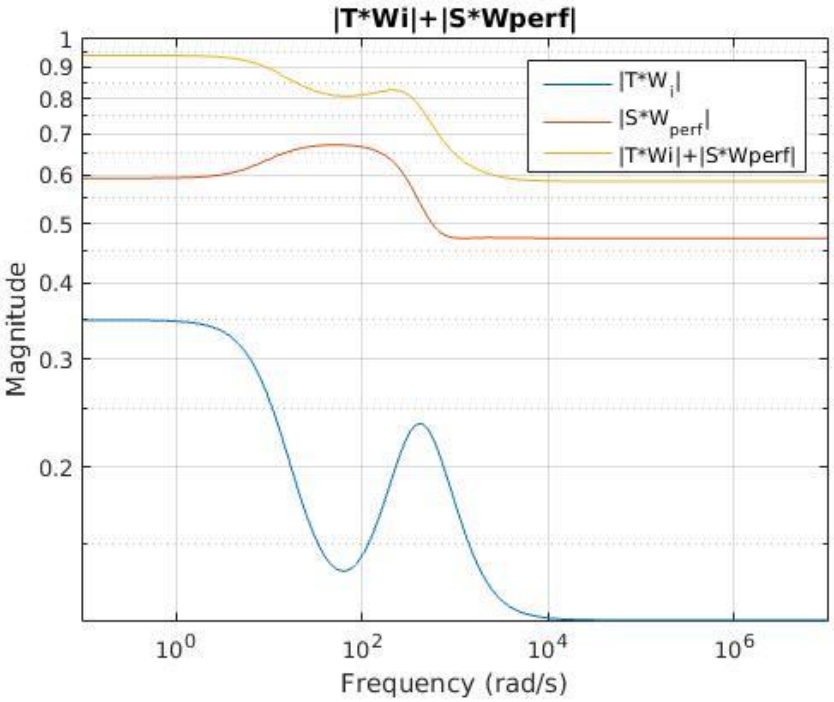

Figure 16: |Wi T|+|Wp S|

Method 2: Structured singular value analysis

The performance can be defined in terms of weighted sensitivity and thus the robust performance of the system can be analyzed by augmenting the output of the system with a

performance weightage, W_p and introducing a w to the output as shown in figure 17 below. The block diagram in figure 17 can be rearranged into the NΔ – structure as shown in figure 18 below.

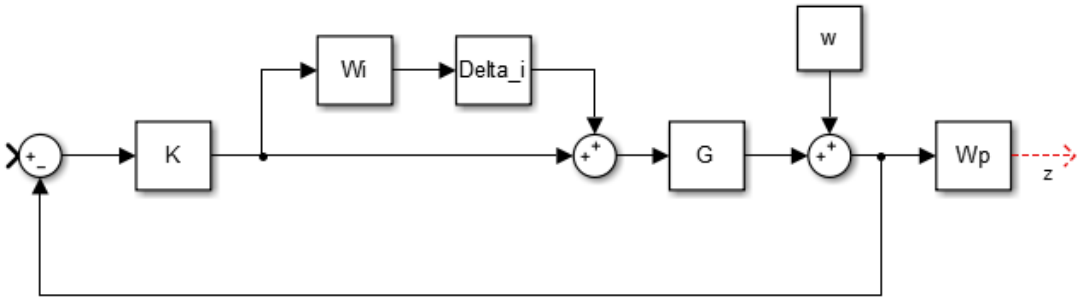

Figure 17: RP of system with input uncertainty

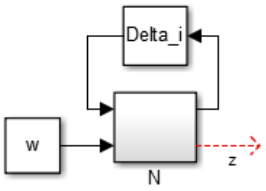

Figure 18: NΔ – structure

Setting,

$$\hat{\Delta} = \begin{bmatrix} \Delta_i & 0 \\ 0 & \Delta_P \end{bmatrix} \quad (33)$$

For the system to satisfy robust performance, we will need the structured singular value, $\mu_{\hat{\Delta}}(N)$ to be smaller than 1 for all frequency. A Simulink model is then constructed and the maximum structured singular value is analyzed for the broken loop single loop at a time and for both loop together.

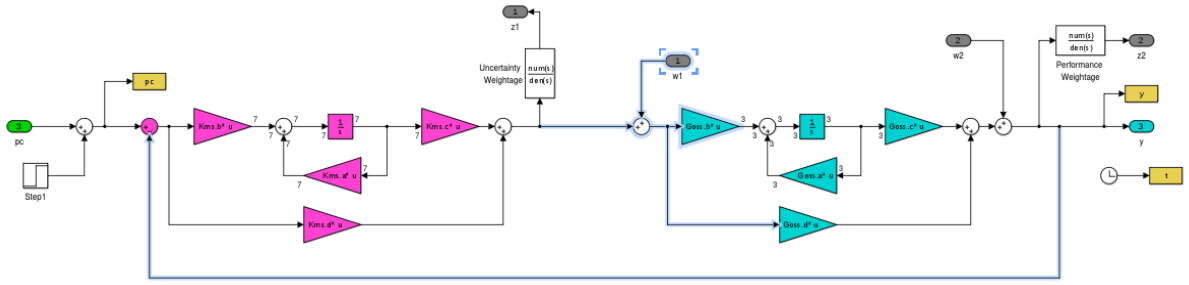

Figure 19 : Simulink diagram

From the previous analysis, the designed controller is able to satisfy both the nominal performance and robust stability requirement. This is again verified by the structured singular value for the broken loop single loop at a time analysis.

The structured singular value for both loop together is also below the upper bound of 1 which verify our previous results. The designed system is able to satisfy the robust performance criteria.

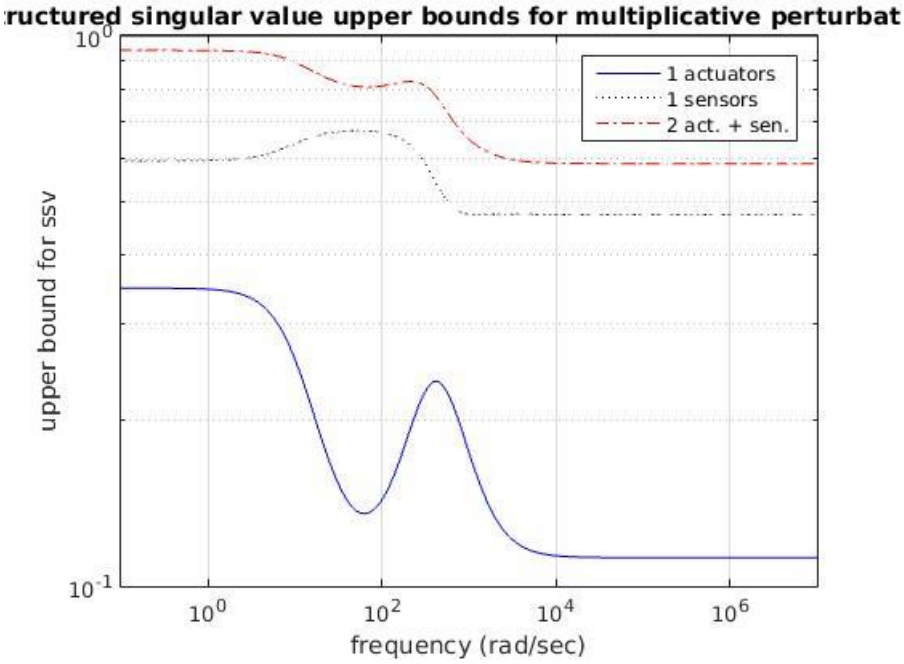

Figure 20: Structured singular value analysis with upper bound of 1

The maximum structured singular value for each case is as listed in table 6 below. The maximum structured singular value satisfied our upper bound of 1.

Loop	Frequency (rad/s)	Maximum μ
u (single loop at a time)	0.0100	0.35
y (single loop at a time)	44.1119	0.68
u and y	0.0100	0.94

Table 6: Maximum structured value

Based on the Simulink diagram in figure 19, the interconnection matrix is constructed and as shown in equation 34 below.

$$\mathrm{M} = \begin{bmatrix} W_I T_I & W_I K S \\ W_P S G & W_P S \end{bmatrix} \quad (34)$$

where $T_I = KG(1+KG)^{-1}$,$S = (1+GK)^{-1}$.

Thus the RP condition for this SISO system holds as

$$\mu(M) = \mu\begin{bmatrix} W_I T_I & W_I K S \\ W_P S G & W_P S \end{bmatrix} = \mu\begin{bmatrix} W_I T_I & W_I T_I \\ W_P S & W_P S \end{bmatrix} = |W_i T| + |W_p S| \quad (35)$$

$$max_\omega\left(|W_i T| + |W_p S|\right) = 0.94$$

Therefore, the robust performance is satisfied which matches the findings from method 1.

Reference

[1] Overview of Missile Flight Control Systems, Paul B. Jackson, Johns Hopkins Apl Technical Digest, Volume 29, Number 1, 2010

[2] Missile Longitudinal Autopilots: Connections Between Optimal Control and Classical Topologies, AIAA Guidance, Navigation, and Control Conference and Exhibit, 15 - 18 August 2005

[3] R.T. Reichert, "Robust Autopilot Design Using μ-Synthesis", American Control Conference, 1990

[4] PaulZarchan. Tactical and Strategic Missile Guidance, fifth Edition [M].Lexington: AIAA Inc., 2005.

[5] F Wiliam Nesline, Paul Zarchan. Why modern controller scan go unstable in practice [J]. AIAA, 1984, 7(4): 495~500.

[6] F William Nesline, Mark L Nesline. How autopilot requirements constrain the aerodynamic design of homing missiles [C]. American Control Conference, San Diego, 1984: 716~730.

[7] S. Skogestad and I. Postlethwaite, Multivariable Feedback Control. Chichester, England: John Wiley & Sons, 1996.